The selective oxidation of methanol to formaldehyde on iron molybdate catalysts and on component oxides

M. Bowker *, R. Holroyd [a], A. Elliott, P. Morrall, A. Alouche [b], C. Entwistle [c] and A. Toerncrona [d]

Department of Chemistry, University of Reading, Whiteknights, Reading RG6 6AD, England
[a] *Now at VG Scientific, East Grinstead, UK*
[b] *Chem. Dept., Al-Baath University, Syria*
[c] *Now at Chemistry Dept., Univ. Durham, England*
[d] *Perstorp AB, S-284 80, Perstorp, Sweden*

Received 27 June 2002; accepted 27 June 2002

The reaction of methanol with an industrial iron molybdate catalyst, and with Fe_2O_3 and with MoO_3, has been investigated with a pulsed flow reactor and temperature-programmed desorption (TPD). The molybdena-based samples show only formaldehyde in TPD as the carbon-containing product, arising from the decomposition of a surface methoxy species. In contrast, haematite yields no formaldehyde, only CO_2 and H_2, which evolve coincidently at 290 °C, and indicates the presence of a formate intermediate on the surface. In turn, the reactor work shows high selectivity to formaldehyde for the molybdate materials and zero for haematite. The iron molybdate sample is more active than the molybdena, conversion beginning at 150 °C for the former and 270 °C for the latter. These data are discussed in terms of a global mechanism for the reaction and a tentative reaction enthalpy profile is proposed. The main differences between the iron and molybdenum samples arise from the stronger binding of oxygen in the former and the higher concentration of cation sites.

KEY WORDS: temperature-programmed desorption; formaldehyde; industrial iron molybdate catalyst.

1. Introduction

The first industrial processes for production of formalin, *i.e.*, an aqueous solution of formaldehyde, was based on oxidative dehydrogenation of methanol over a copper catalyst. Improvements in catalyst technology resulted in substitution of the copper catalyst for an unsupported silver catalyst, which is the formula still used today. In the 1950s a competing process for production of formaldehyde was developed. This process was based on selective (partial) oxidation of methanol over an Fe–Mo oxide catalyst. The two processes, referred to as silver and oxide processes respectively, are used today for production of formalin on the industrial scale. Each process accounts for about 50% of the total production of formalin, which today amounts to about 20 Mton per annum, expressed as 37% HCHO in water.

Although both processes account for roughly an equal part of the total formalin production, it is clear that most of the new capacity that has been taken into operation during the last 10 years is based on the oxide process. Formaldehyde is used to produce different resins, *e.g.*, for MDF-boards (medium dense fiber), thermosetting plastics such as bakelite, laminate flooring and polyalcohols.

The conditions under which the Ag and oxide catalysts operate are somewhat different, especially in terms of oxygen to methanol ratio (Ag operates with less air and involves the overall reactions A and C below, whereas the molybdate works mainly through reaction C), and temperature (*ca* 650 °C for Ag and 350 °C). The silver process operates at a methanol/air ratio above the upper explosion limit (net reducing gas mixture), whereas the oxide process operates at a methanol/air ratio below the lower explosion limit (net oxidizing gas mixture). The main reactions to be considered here are the following:

Dehydrogenation

$$CH_3OH \rightarrow H_2CO + H_2 \qquad (A)$$

$$\Delta H = 84\,\mathrm{kJ\,mol^{-1}}$$

$$CH_3OH \rightarrow CO + 2H_2 \qquad (B)$$

$$\Delta H = 97\,\mathrm{kJ\,mol^{-1}}$$

Oxidative dehydrogenation

$$CH_3OH + \tfrac{1}{2}O_2 \rightarrow H_2CO + H_2O \qquad (C)$$

$$\Delta H = -159\,\mathrm{kJ\,mol^{-1}}$$

Combustion

$$CH_3OH + 1\tfrac{1}{2}O_2 \rightarrow CO_2 + 2H_2O \qquad (D)$$

$$\Delta H = -674\,\mathrm{kJ\,mol^{-1}}$$

* To whom correspondence should be addressed.
E-mail: m.bowker@rdg.ac.uk

1011-372X/02/1100-0165/0

$$CH_3OH + O_2 \rightarrow CO + 2H_2O \quad (E)$$

$$\Delta H = -389\,kJ\,mol^{-1}.$$

As for all selective oxidation reactions, step C is affected by loss of efficiency due to combustion of the reactants to CO_2 and water, which is more thermodynamically favored. We have carried out a considerable amount of work on methanol oxidation, most of it on well-defined surfaces of Cu [1–4], from which a complete mechanism for the reaction on that surface has evolved. The steps are as follows, where subscript a refers to adsorbed species:

$$CH_3OH \rightarrow CH_3OH_a \quad (1)$$

$$O_2 \rightarrow 2O_a \quad (2)$$

$$CH_3OH_a + O_a \rightarrow CH_3O_a + OH_a \quad (3)$$

$$CH_3OH_a + OH_a \rightarrow CH_3O_a + H_2O \quad (4)$$

$$CH_3O_a \rightarrow H_2CO_a + H_a \quad (5)$$

$$2H_a \rightarrow H_2 \quad (6)$$

$$H_a + OH_a \rightarrow H_2O \quad (7)$$

$$H_2CO_a \rightarrow H_2CO. \quad (8)$$

The reactivity of the oxygen-dosed surface was high (the reaction probability for methanol is 0.2 [3]), but no reaction was evident in these low-pressure experiments in the absence of chemisorbed oxygen atoms. Besides this selective oxidation route, combustion can occur on Cu by the following steps:

$$H_2CO_a + O_a \rightarrow H_2COO_a \quad (9)$$

$$H_2COO_a \rightarrow HCOO_a + H_a \quad (10)$$

$$HCOO_a \rightarrow CO_{2g} + H_a \quad (11)$$

$$H_a + O_a \rightarrow OH_a \quad (12)$$

$$OH_a + H_a \rightarrow H_2O_g. \quad (13)$$

It is from this mechanistic basis that we were interested in determining how the reaction proceeds on iron molybdate catalysts. The reaction on iron molybdate is only infrequently reported in the literature, but it is known that the best industrial catalysts consist of a mixed phase of ferric molybdate [$Fe_2(MoO_4)_3$] and molybdena [MoO_3]. Generally, the reaction is considered to be of the redox type, with the oxygen of the catalysts participating in the reaction [5], and with activation energies reported to be in the range 70–90 kJ mol^{-1}. However, there are a number of questions which remain unanswered, such as, what is the role of the separate phases and elements in these catalysts? It has been suggested that the major active phase is the iron molybdate, with the excess Mo only adding to the structural properties of the catalyst (increasing surface area and maintaining adequate Mo levels) [6], though there is some evidence for synergy between these components, *i.e.*, higher activity for the mix compared with the individual components [7]. A further question which remains contentious is the nature of the rate-determining step (RDS) in the reaction. Several steps have been postulated as rate-determining, including desorption of the products [8], re-oxidation of the surface [5] and the reaction of methanol with surface oxygen [9]. A pulsed-flow experiment did result in higher conversions than observed during continuous flow and this was attributed to slow product desorption [8]. A kinetic study by Machiels and Sleight addressed some of these points [10]. They confirmed the redox nature of the reaction using isotope labeling and proposed that the mechanism involved reversible, dissociative adsorption of methanol, forming methoxy groups. The RDS was proposed to be the methoxy dehydrogenation to produce formaldehyde.

These points are addressed in more detail in this work, which uses transient methods to examine the reaction on iron molybdate and its component oxides.

2. Experimental

The experiments were carried out on two main pieces of equipment—a home-built pulsed-flow reactor and a small vacuum system for TPD measurements. The former has been reported elsewhere [11] but can briefly be described as follows. It consists of a gas-supply system and a facility for pulsing gases *via* automatic repetitive sample valve firing. However, for pulsing a liquid like methanol manual injections of 3 μl of the liquid are periodically injected into an O_2/He flow (50 ml/min, O_2:He = 3:4). At these flows this produced a methanol pulse with a width of ~24 s, much wider than that for pulsed gases which typically have a width of ~5 s. The reactants/products were detected in real time with an on-line mass spectrometer system using a HIDEN IV quadrupole mass spectrometer. Some of the TPD results were obtained in a high vacuum chamber with a base pressure of 10^{-8} mbar. A VG QX200 mass spectrometer was used to detect desorbed products after the adsorption of various reactants. TPD was also obtained in the pulsed-flow reactor after dosing at room temperature, heating at a rate of 20 °C min^{-1} in 50 ml min^{-1} of He flow. We should note here one of the problems associated with mass spectrometric analysis of such reactions and this can be seen in the result figures, *e.g.*, figure 4. It can be seen that the 30 amu signal seen when methanol is pulsed is about 65% of the 31 amu signal, the latter being the major cracking fragment for methanol. The true cracking fraction ratio 30:31 should be about 10%. The reason for this is that the mass spectrometer filament itself acts as a catalyst,

as evidenced from experiments bypassing the real catalyst, which still show cracking and oxidation products (such as CO_2). It can be seen in figure 4, however, that above 150 °C mass 31 declines due to conversion of the methanol on the catalyst, while mass 30 increases due to formaldehyde production. Thus the contribution of the filament can be estimated and, although raw data is shown in the direct pulsed flow data (*e.g.*, figure 4), the selectivities and conversions (*e.g.*, figure 5) have been corrected for this effect.

The catalytic samples used were MoO_3 (BDH, AnalaR), Fe_2O_3 (Aldrich) and several industrial catalysts produced by Perstorp. The Mo/Fe molar ratio in the catalyst used is about 2.2. The catalyst is prepared by coprecipitation of aqueous solutions of Fe(III) and Mo(VI). The resulting dried precipitate is shaped into hollow-tablets and is calcined. Several catalysts were examined, including those unloaded from several positions in a commercial plant, but only work on the unused catalyst will be reported here, in comparison to the monometallic oxides. The catalyst pellets were broken up before use, crushed and sieved, and only granules greater than 0.6 mm diameter were used in order to avoid reactor blocking. The same-sized granules of the other oxides were also used.

The methanol was BDH, AnalaR (99.8%).

The surface areas of the various samples were determined by BET and are $7\,m^2\,g^{-1}$ for the Perstorp sample, $6\,m^2\,g^{-1}$ for the MoO_3 and $10\,m^2\,g^{-1}$ for the Fe_2O_3. The XRD bulk structures were as expected for the single oxide samples (Fe_2O_3 [12], MoO_3 [13]). The Perstorp sample showed a diffractogram to be expected for a mixture of orthorhombic MoO_3 [13] and monoclinic iron molybdate, $Fe_2(MoO_4)_3$ [14].

3. Results

3.1. TPD

TPD data are shown in figures 1–3. The iron molybdate catalyst shows a broad desorption of water in two peaks at 100 °C and 200 °C. The former is near-coincident with methanol desorption, which is essentially complete by 200 °C. Coincident with the second peak at 190 °C is formaldehyde, which represents the vast majority of the organic evolved. Using the Redhead formula [15] for the relationship between peak temperature and activation energy for the surface process gives the result shown in table 1. The water desorption is broad and slow and is not complete even at 300 °C, while the formaldehyde is complete by 240 °C. The tailing on the water may be due to re-adsorption of water in the catalyst bed, or due to the second-order nature of water formation from hydrogen and hydroxyl groups.

This desorption profile is in stark contrast to that from Fe_2O_3 shown in figure 2, which shows no selectivity to formaldehyde. The main product is CO_2 at 300 °C, with near-coincident hydrogen. The hydrogen also has a first, broad desorption peak at 200 °C, followed by the second peak at 290 °C, near-coincident with CO_2. The only other desorption is a small amount of methanol at 90 °C, and a broad water peak at 110 °C. There is no evidence of formaldehyde evolution. The CO_2 is likely to be the result of formate decomposition and the peak shape is first order. The peak temperature yields a desorption energy of $163\,kJ\,mol^{-1}$, as shown in table 1.

There is very little desorption from the MoO_3 sample as shown in figure 3. There is a small desorption peak at around 70 °C, and formaldehyde evolves at 200 °C.

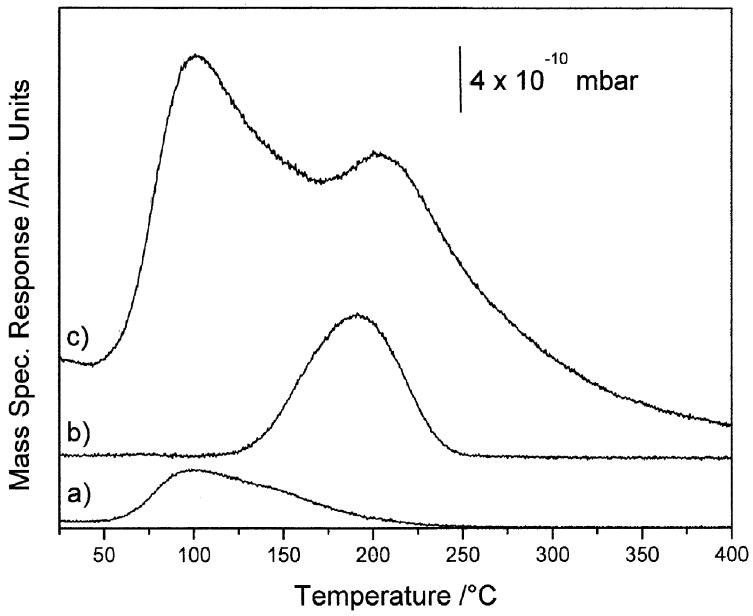

Figure 1. TPD from the Perstorp sample after dosing 36 μl of methanol at 25 °C. The products are water and formaldehyde. (a) 31 amu (methanol); (b) 30 amu (formaldehyde, contribution from methanol subtracted) and (c) 18 amu (water).

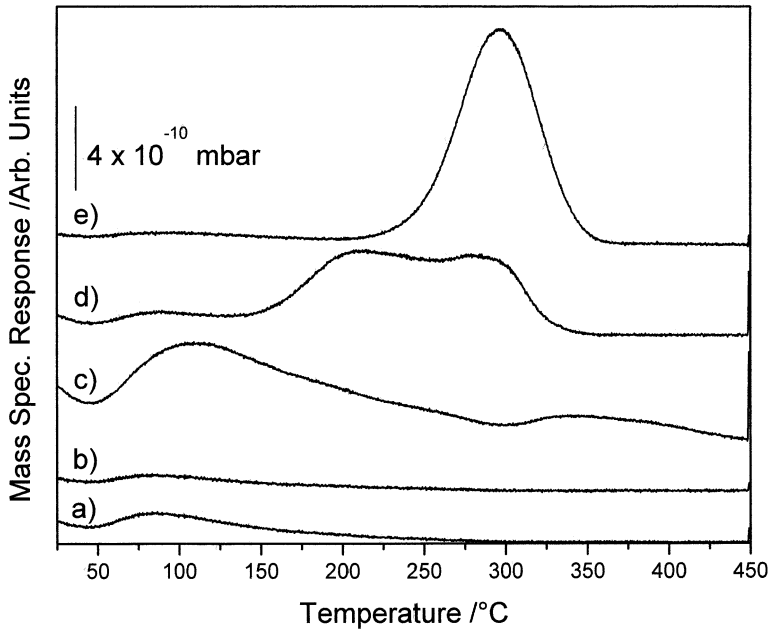

Figure 2. TPD from Fe_2O_3 after dosing 36 μl of methanol at 25 °C. The products are CO_2, H_2 and H_2O. As in figure 1, plus (c) 18 amu × 0.5, (d) 2 amu (hydrogen) and (e) 44 amu (carbon dioxide).

Water evolution is difficult to identify from the background, for such a small amount of total adsorption. Thus, the MoO_3 sample shows good selectivity to formaldehyde, but with reduced adsorption activity.

Some limited experiments were carried out with other related adsorbates. Formaldehyde was dosed onto the Perstorp catalyst and showed a low temperature of desorption beginning immediately upon heating, with a peak at 50 °C, well below the temperature for formaldehyde evolution from methanol adsorption. Thus, formaldehyde desorption in the latter case is reaction limited, not desorption limited. Similarly formic acid was dosed in order to examine its stability and decomposition products. It adsorbed efficiently and evolved H_2 and CO_2 at 25–130 °C, while CO and H_2O evolved between 80 and 180 °C; thus dehydrogenation and dehydration pathways occur, probably via different types of formate intermediates. Since this pathway is so facile it is clear that the formate is not accessed by room temperature methanol adsorption on this material.

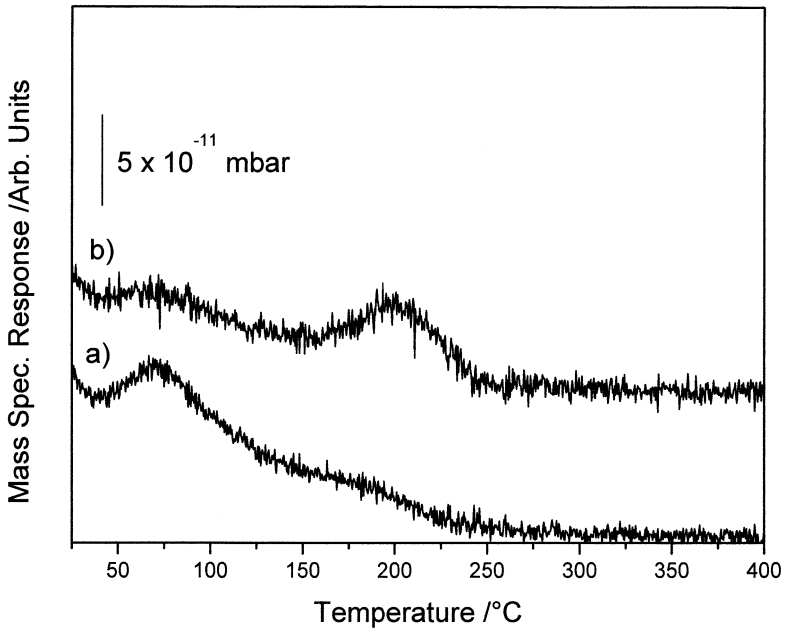

Figure 3. TPD from MoO_3 after dosing 36 μl of methanol at 25 °C. The main products are formaldehyde and water, but note that very little methanol was adsorbed. Labels as for figure 1.

Table 1
Estimated activation energies for surface intermediate decomposition.

Catalyst	Surface process	Value ($kJ\,mol^{-1}$)
Perstorp	Methoxy decomposition	132
Fe_2O_3	Formate decomposition	163
MoO_3	Methoxy decomposition	135

Note: Desorption of methanol from all catalysts occurs with an activation energy of about $100\,kJ\,mol^{-1}$.

In the following section, the pulsed-flow reaction results are presented in comparison to these data.

3.2. Pulsed-flow reactor

Figure 4 shows a temperature-programmed pulsed-flow reaction profile for the Perstorp iron molybdate catalyst. The reaction begins at around 180 °C, with methanol conversion being almost complete by 230 °C, and the formaldehyde selectivity being very high up to 220 °C (figure 5(a)) at about 100%. The formaldehyde yield peaks at about 290 °C, while CO and CO_2 evolution become high by 300 °C. The major products at 400 °C are CO, CO_2 and water, with high selectivity to CO and only small amounts of hydrogen. Experiments were carried out with varying levels of oxygen in the feed with the result that dehydrogenation of the methanol became dominant at high temperature. With zero oxygen, conversion of methanol began at slightly higher temperature and was complete by about 350 °C (figure 5(b)). Formaldehyde selectivity was very high up to 320 °C. At 400 °C the products were CO, CO_2 and H_2O, with a high yield of hydrogen. The selectivity plots in figure 5 show that CO is the dominant product at high temperature. Minor products were checked for and the only one positively identified was dimethyl ether, present at 2% maximum selectivity. Note that the product distribution in the absence of oxygen is important in relation to a recent patent describing the regeneration of formaldehyde synthesis catalysts using methanol as a reductant of decayed samples [7]. Detailed analysis of the shapes of the product curve will not be given here, but there is clearly some complexity in the CO and CO_2 evolution, as evidenced by the presence of a double peak in the evolution curves for the latter (200–320 °C) and the broadening of the former (190–220 °C).

The reaction profile for MoO_3 is different, in particular the sample is less active than the iron molybdate. The reaction only begins at around 270 °C (figure 6) and methanol conversion is never complete, even at 400 °C. On the other hand, the selectivity to formaldehyde is very high, even at high temperature, and the main oxidized product is CO_2. The selectivity profile is given in figure 7(a). In the absence of gas-phase oxygen, conversion is delayed, starting at about 290 °C and reaching 90% by 390 °C (figure 7(b)). Significant formaldehyde

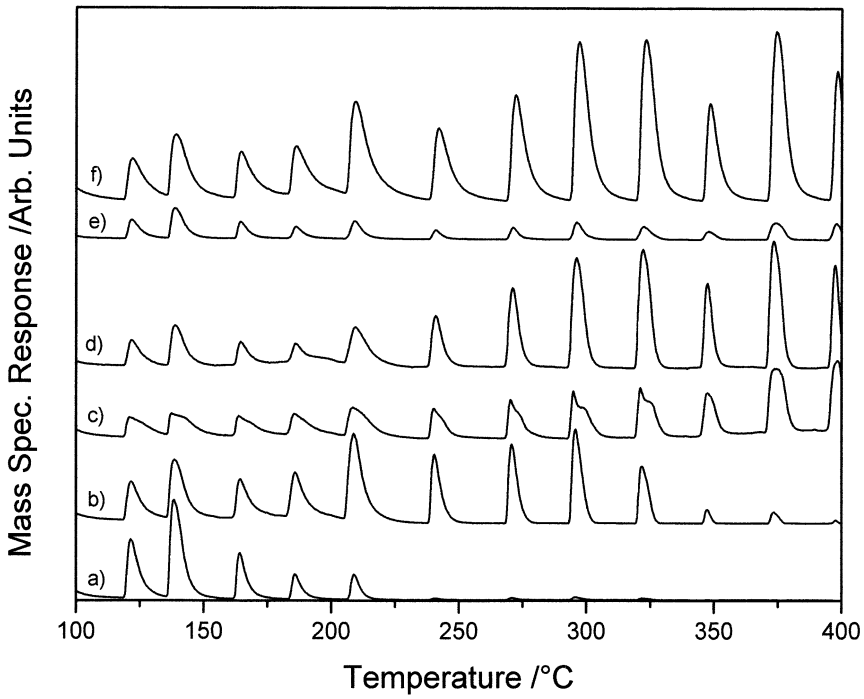

Figure 4. Temperature-programmed pulsed-flow reaction of methanol with oxygen over the Perstorp catalyst. The main features to be observed are the loss of methanol at very low temperature, the production of formaldehyde in the middle temperature range (200 °C to 320 °C), and the production of CO at high temperatures. (a) 31 amu (methanol); (b) 30 amu (formaldehyde, but note the significant contribution from methanol at low temperature, due to reaction on the mass spectrometer filament); (c) 44 amu (carbon dioxide); (d) 28 amu × 0.5; (e) 2 amu × 0.33 (hydrogen) and (f) 18 amu × 0.33 (water).

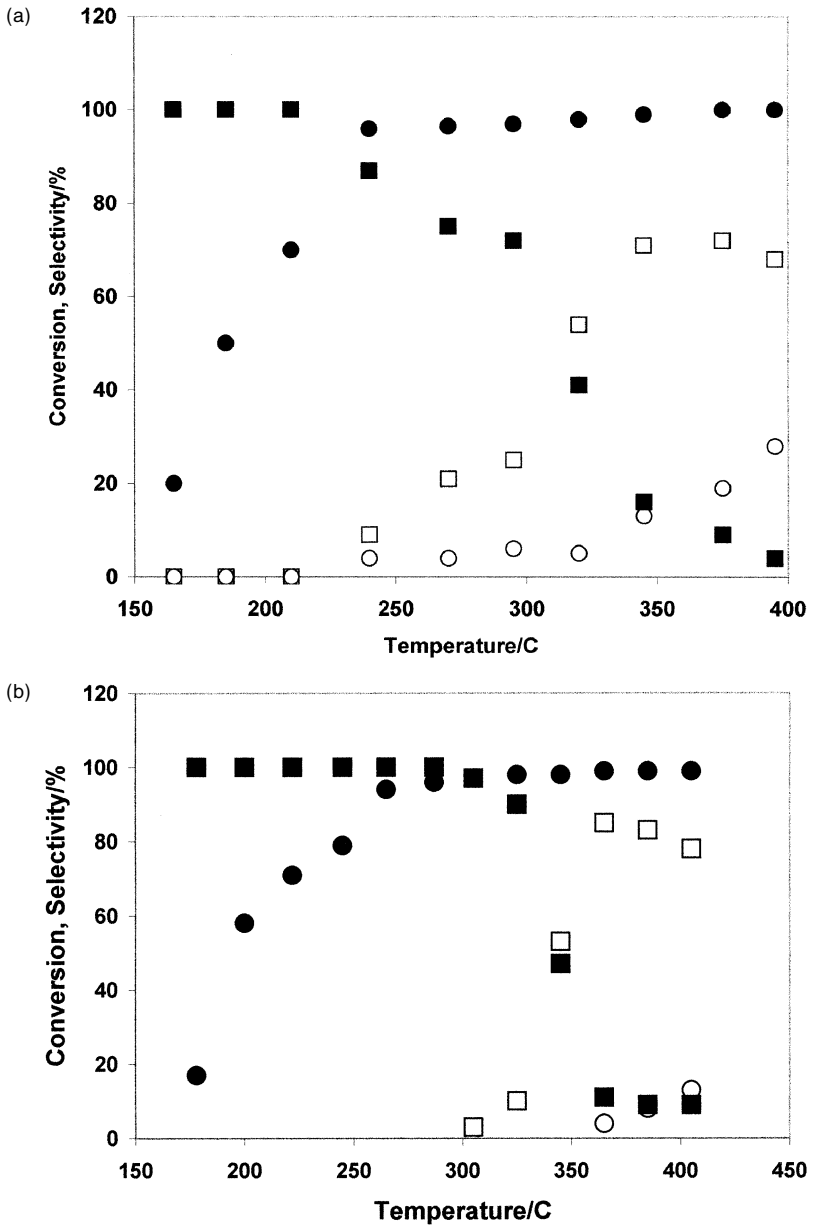

Figure 5. Conversions and selectivities for the methanol oxidation over the Perstorp sample (a) in the presence of oxygen, as in figure 4, and (b) in the absence of oxygen. ●, methanol conversion; ■, formaldehyde selectivity; □, CO and ○, CO_2.

production occurs at around 350 °C, but CO, H_2 and water are dominant products at 400 °C.

The behavior of Fe_2O_3 contrasts strongly with these data. As can be seen in figure 8, methanol conversion only begins at about 250 °C and is complete by 320 °C. With the beginning of the conversion it is apparent that the CO_2 profile is very broad and severely lags the input pulse. As temperature increases, the width of the CO_2 diminishes until it is near coincident with the other products at 400 °C. There is little evidence for formaldehyde production in this case; instead CO_2, water and hydrogen are the dominant products, with little evidence of any CO production (figure 9(a)). In the absence of oxygen in the gas phase, conversion begins at 280 °C and is complete by approximately 370 °C. Again CO_2 is the dominant product at high temperature, with much less water production and little evidence of CO (figure 9(b)). The lack of CO production implies that combustion occurs through the formate intermediate and that clean dehydrogenation does not occur on haematite to any significant degree under these conditions.

4. Discussion

Comparative plots of the behavior of these different materials is given in figure 10(a), (b), (c) and (d), and

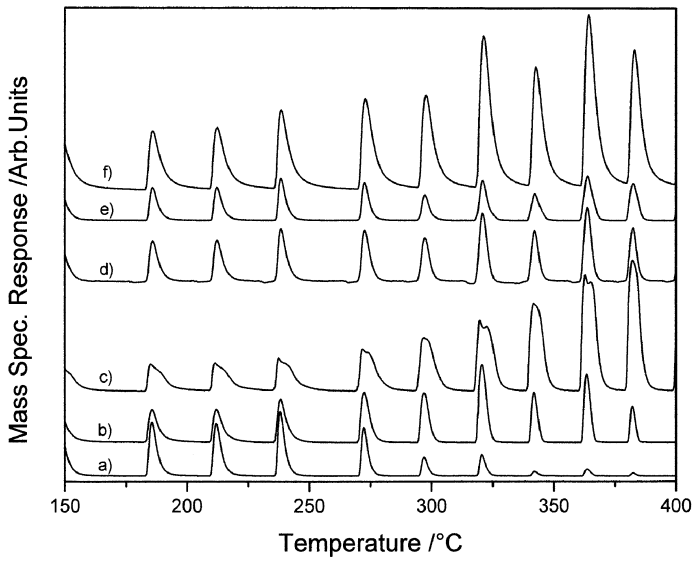

Figure 6. Temperature-programmed pulsed-flow reaction of methanol and oxygen over the molybdena catalyst. Note the higher temperature of conversion compared with figure 4, and higher selectivity to formaldehyde at high temperature. Labels as in figure 4, except (a) and (b) are $\times 0.5$.

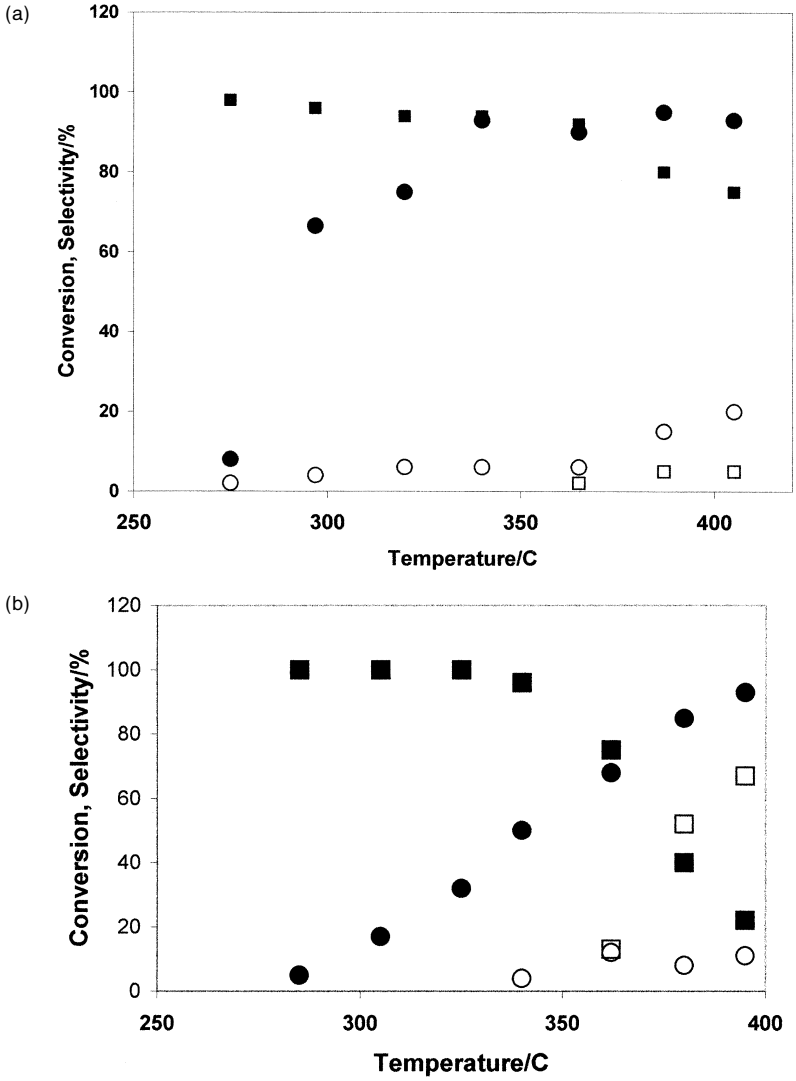

Figure 7. Conversions and selectivities for the methanol oxidation over the molybdena sample (a) in the presence of oxygen, as in figure 4, and (b) in the absence of oxygen. Symbols as in figure 5.

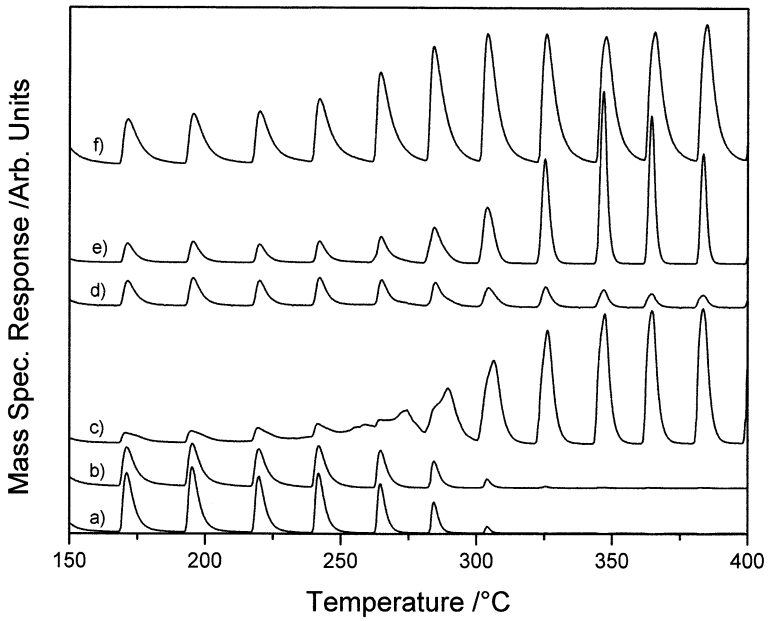

Figure 8. Temperature-programmed pulsed-flow reaction of methanol and oxygen over the haematite catalyst. Here no formaldehyde production is observed. Labels as in figure 4, except (c) which is $\times 0.5$.

several features of this catalytic system are clear from these data.

Fe_2O_3 is a combustor of methanol. Both the pulsed-flow reactor and TPD results bear this out. It is clear from the TPD that the species which decomposes to produce CO_2 and H_2 at 300 °C is probably also responsible for some self-poisoning of the iron oxide surface in the pulsed-flow reactor measurements. This is indicated by the very slow CO_2 evolution after the pulses where conversion is just beginning (figure 6). This species is most likely to be the formate species, which is also produced on copper surfaces in experiments with CH_3OH/O_2 mixtures [16,17]. This formate is likely to be bidentate and so stable that it blocks methanol reaction until *ca* 250 °C, a much higher temperature than for the Perstorp sample, even though the iron oxide is intrinsically very active (100% conversion by 320 °C and a large extent of adsorption measured by TPD).

On the other hand, the molybdate materials are highly selective, with molybdena itself being surprisingly so. In TPD there is hardly any sign of CO_2 production and formate formation. It is likely that the major intermediate present on these materials is the methoxy species, which decomposes at about 190 °C to produce formaldehyde, and methoxy has been identified on MoO_3 using IR spectroscopy after methanol dosing [18,19]. The non-selective component on molybdena is deep oxidation to CO_2, which is not the case with the Perstorp sample. Further, the Perstorp catalyst is apparently much more active than molybdena or iron oxide. It should also be noted, however, that the behavior of the industrial catalyst is affected by the length of time on-line in the full-scale plant, and its position in the bed [7,20].

In the absence of oxygen, it is clear that, at least in a single run, the Perstorp catalyst characteristics are still largely maintained, but shifted to higher temperatures. There is much more hydrogen production as also observed for the other two catalysts. The iron oxide sample produces mainly CO_2 and hydrogen, probably through the formate whose presence is identified in TPD in the absence of gas-phase oxygen. The molybdena produces much more CO in the absence of oxygen.

Clearly, it would be a disaster for an industrial catalyst's performance if iron oxide were present in the catalyst, and there is little doubt that one reason for an excess of molybdena in the industrial sample is to avoid the appearance of free Fe oxide. This is analogous to the excess of Sb used in the $FeSbO_4$-type catalyst used for propene ammoxidation, as described by Boreskov *et al*. [21]. Further, it has been proposed for the latter types of catalyst that it is important to dilute the cation associated with combustion pathways in the final materials [22]. Again it is likely that the same hypothesis pertains here and that the surface configuration of the industrial catalyst ensures a minimal number of adjacent Fe–Fe cation sites. Indeed, it has been proposed that for $FeSbO_4$-type catalysts, the surface may be entirely dominated by Sb [23]. It is evident that molybdena is highly selective for formaldehyde, but its activity is more limited than the iron molybdate. The enhanced performance could either be due to a changed stability of the surface oxygen atoms or improved diffusivity of oxygen anions within the lattice. That the surface oxygen atoms are the active species is clear from the

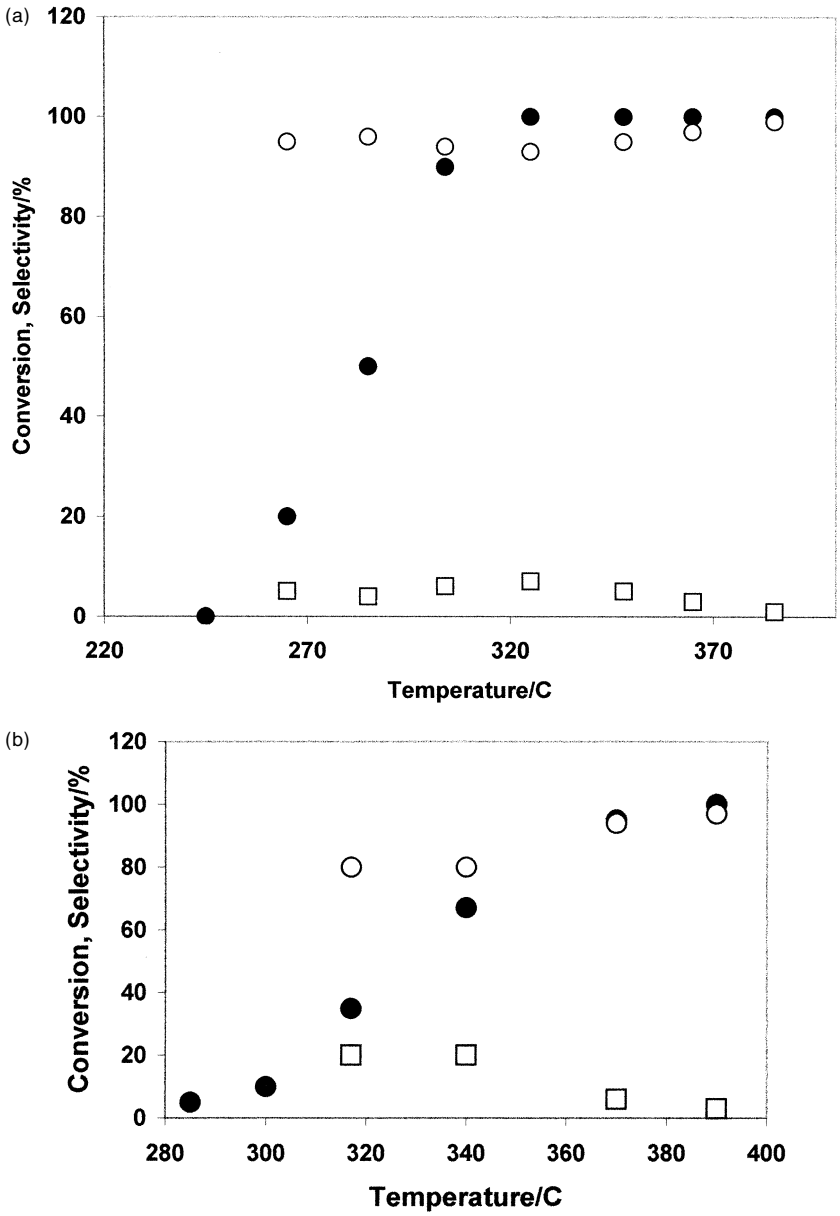

Figure 9. Conversions and selectivities for the methanol oxidation over the haemetite sample (a) in the presence of oxygen, as in figure 4, and (b) in the absence of oxygen. Symbols as in figure 5.

anaerobic reactions, where broadly similar reaction patterns are seen to be those in the presence of oxygen. The anaerobic reactions also show that oxygen is mobile within the lattice because in experiments of the type shown in figure 4, but without the presence of gas-phase oxygen, the pulses involved produce 7×10^{20} molecules of water, equivalent to approximately 20 monolayers of oxygen cations. Thus, sub-monolayer oxygen must diffuse to the surface during these reactions. However, one final question is why the reaction temperature is a little higher in the absence of oxygen. The most likely reason is an imbalance of population of the methoxy and oxygen anion, *i.e.*, over-population by methoxy species and under-population by oxygen anions. This, in turn, could indicate a limited mobility of anions at low temperature.

In terms of the mechanistic steps given in the introduction, we can make certain deductions about the reaction pathway of these different surfaces, and this refers to figure 11, which is a hypothetical potential energy pathway for the reaction. Since formaldehyde is not seen from iron oxide it is clear that it is easy on that surface to make the formate and that decomposition of this species may be rate limiting, since it is quite stable. Thus, in figure 11 we have shown low barriers from gas-phase methanol to the formate *via* adsorbed formaldehyde. We have assumed that the pathway goes *via* this intermediate and that formate is not formed by

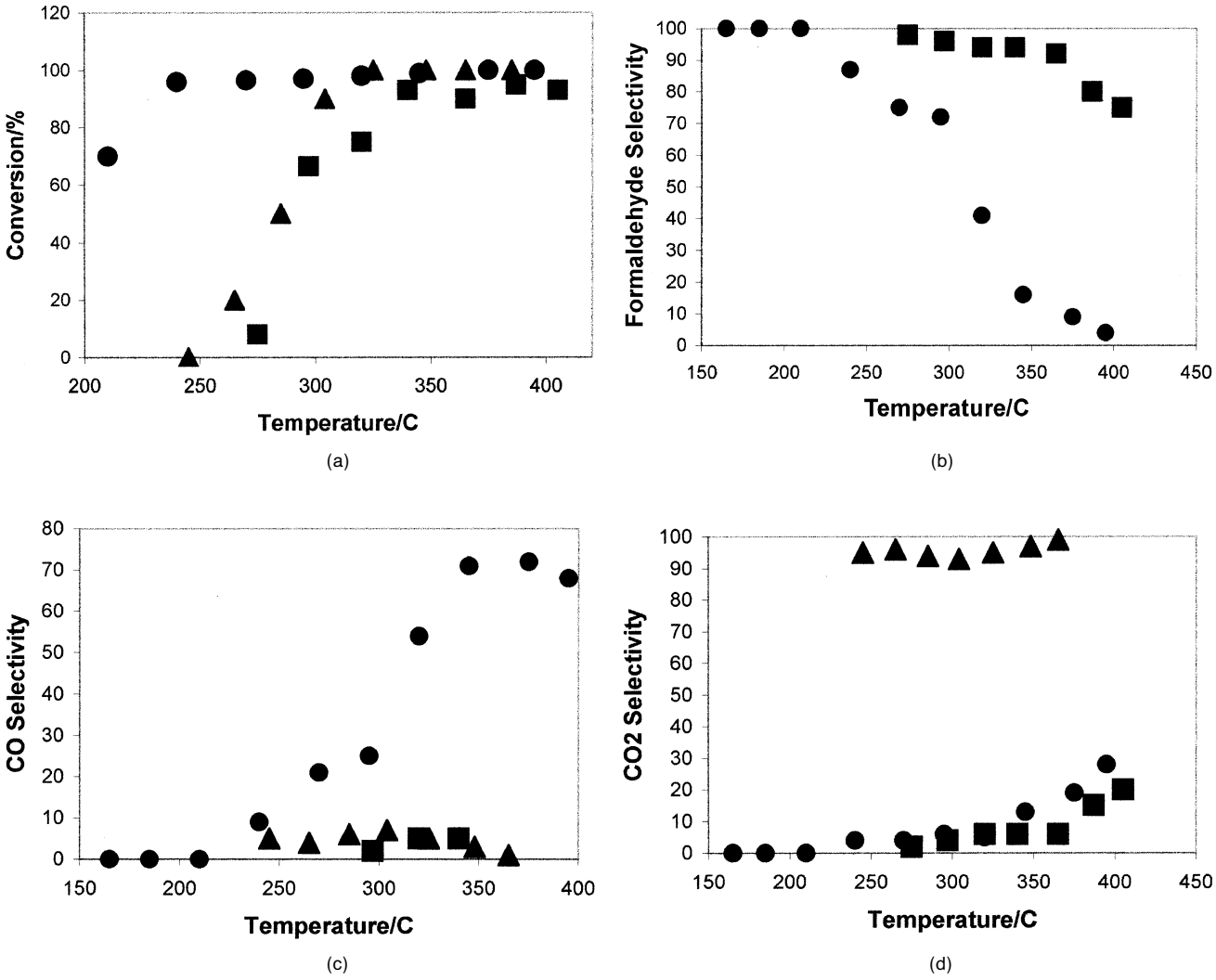

Figure 10. Comparative plots of the performance of the different catalysts used for methanol oxidation in this work. (a) Conversion (●, Perstorp; ▲, iron oxide; ■, molybdena); (b) formaldehyde selectivity; (c) CO selectivities and (d) CO_2 selectivities.

formaldehyde production and re-adsorption. On molybdena the barriers to formaldehyde in the gas phase are relatively low, but those for further reaction are higher than on iron oxide. For the Perstorp catalyst the pathway is similar but has a low energy pathway to formaldehyde, largely due to a decreased barrier to methanol adsorption in our scheme. This is proposed because the formaldehyde peak in the TPD for MoO_3 is at about the same temperature as for the Perstorp catalyst (it is actually slightly higher in temperature), but the extent of adsorption for the same dose is much lower (by about a factor of about 10). That difference amounts to a difference of about $6\,kJ\,mol^{-1}$ in the adsorption term. Because of the stronger binding of oxygen on iron oxide the reaction pathway passes through a lower enthalpy situation, which therefore produces a higher barrier to the appearance of formaldehyde in the gas phase, and the route to formate and combustion is therefore favored. It should be stated that figure 11 is tentative since some of the detailed numbers for kinetic steps are missing, and not every single step is shown. Importantly, it is likely that the kinetics of these processes will be morphology dependent, and detailed surface science studies of the crystal plane variation of these reactions would be helpful in this respect. This working scheme of the reaction needs other detailed experiments to give good quantification to the plot, as outlined below.

A further remaining question is why the formate is so readily formed on iron oxide but not on the molybdenum-based materials. The most likely explanation is that, because the oxygen on the iron oxide surface is much more strongly bound than on the other materials, formate formation and burning is facilitated. In turn this is due to the low enthalpy of these intermediates on that surface, their "deep" oxidation and their proximity in enthalpy to that of the combustion products.

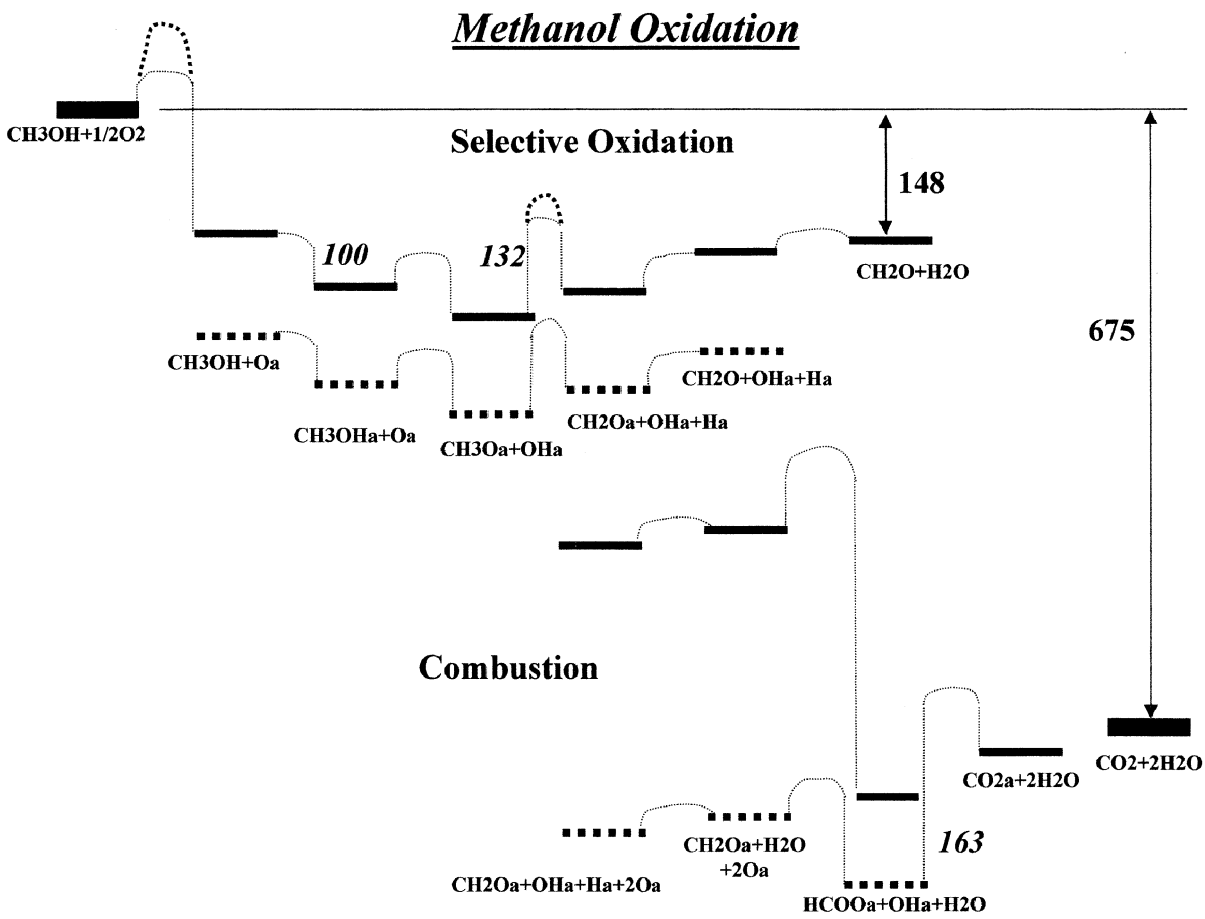

Figure 11. Schematic potential energy profiles for methanol oxidation on the three catalysts studied here. In the upper part of the figure is the selective oxidation pathway, with solid bars representing enthalpies for the iron molybdate and dashed bars are for haematite. Minor differences between molybdena and the iron molybdate samples are shown by bold activation barriers. The steps for haematite are shown generally lower in energy due to the higher enthalpy difference in reduction to the next lowest oxidation state per oxygen atom compared to molybdena (which is approximately 120 kJ mol^{-1} for the bulk materials [24]). Methanol itself adsorbs relatively weakly on metals and oxides, with a small adsorption barrier. Dissociative oxygen adsorption is likely to be activated. The bold numbers are reaction enthalpies; italics are from TPD measurements here. Some of the energetics are estimates only, not all of the individual mechanistic steps are given, and the CO production pathways are not shown.

Thus, from these simple experiments we have learned a great deal about the selective oxidation of methanol on iron molybdate catalysts. In future publications relating to this system we wish to address several problems. These include the extent of oxygen loss from the bulk of these materials during anaerobic and aerobic reaction, the level of steady-state activity under those conditions, and further details regarding the mechanistic steps of the reaction, all in a more quantitative manner.

Acknowledgments

We are grateful for partial support of this work to Perstorp AB and to the British Council for support for a short stay at Reading by A.A.

References

[1] M. Bowker and R.J. Madix, Surface Sci. 95 (1980) 190.
[2] A. Jones, S. Poulston, R.A. Bennett and M. Bowker, Surface Sci. 380 (1997) 31.
[3] C. Barnes, P. Pudney, Q. Guo and M. Bowker, J. Chem. Soc., Faraday Trans. 86 (1990) 2693.
[4] M. Bowker, Topics in Catal. 3 (1996) 461.
[5] P. Jiru, B. Wichterlova and J. Tichy, Proc. 3rd Int. Congr. Catal. I (1965) 199.
[6] M. Carbucchio and F. Trifiro, J. Catal. 45 (1976) 77.
[7] I. Wachs and L. Briand, US patent 6037290 (2000) to Lehigh University.
[8] N. Pernicone, F. Lazzeria, G. Liberti and G. Lanzavecchia, J. Catal. 14 (1969) 293.
[9] B. Popov, K. Osipova, V. Malakhov and A. Kolchin, Kinet. Catal. 12 (1971) 1464.
[10] C. Machiels and A.W. Sleight, 4th Intern. Conf. Molybdenum (1982) 411.
[11] D. Law and M. Bowker, Catal. Today 10 (1991) 397.
[12] JCPDS card 33-0664.
[13] NBS monogr. 25 (1984) 20, 118.
[14] L. Plyasova, J. Struct. Chem. 17 (1976) 647.
[15] P.A. Redhead, Vacuum 12 (1962) 203.
[16] A.H. Jones, S. Poulston, R.A. Bennett and M. Bowker, Surface Sci. 380 (1997) 31.
[17] P. Davies and G. Mariotti, Cat. Letts. 43 (1997) 261.
[18] R. Groff, J. Catal. 86 (1984) 215.

[19] W.-H. Cheng, J. Catal. 158 (1996) 477.
[20] R. Holroyd and M. Bowker, unpublished data.
[21] G.K. Boreskov, V. Shchukin, S. Veniyaminov and D. Tarasova, Kinet. Catal. 11 (1970) 153.
[22] I. Matsuura, Proc. 6th Intern. Cong. Catal. (1976) 819.
[23] M.D. Allen and M. Bowker, Catal. Letts. 33 (1995) 269.
[24] *Handbook of Chemistry and Physics*, 73rd edn (CRC, Boca Raton, 1993), pp. 5–18 and 5–22.